https://doi.org/10.5607/en.2017.26.1.42
Exp Neurobiol. 2017 Feb;26(1):42-54.
pISSN 1226-2560 • eISSN 2093-8144

Original Article

Experimental Neurobiology

Check for updates

Orai1 and Orai3 in Combination with Stim1 Mediate the Majority of Store-operated Calcium Entry in Astrocytes

Jea Kwon[1,2,3], Heeyoung An[1,2,3], Moonsun Sa[1,2,3], Joungha Won[2,3,4], Jeong Im Shin[2,3] and C. Justin Lee[1,2,3]*

[1]KU-KIST Graduate School of Converging Science and Technology, Korea University, Seoul 02841,
[2]Center for Neuroscience and Functional Connectomics, Korea Institute of Science and Technology (KIST), Seoul 02792,
[3]Center for Glia-Neuron Interaction, Korea Institute of Science and Technology (KIST), Seoul 02792,
[4]Department of Biological Science, Korea Advanced Institute of Science and Technology (KAIST), Daejeon 34141, Korea

Astrocytes are non-excitable cells in the brain and their activity largely depends on the intracellular calcium (Ca^{2+}) level. Therefore, maintaining the intracellular Ca^{2+} homeostasis is critical for proper functioning of astrocytes. One of the key regulatory mechanisms of Ca^{2+} homeostasis in astrocytes is the store-operated Ca^{2+} entry (SOCE). This process is mediated by a combination of the Ca^{2+}-store-depletion-sensor, Stim, and the store-operated Ca^{2+}-channels, Orai and TrpC families. Despite the existence of all those families in astrocytes, previous studies have provided conflicting results on the molecular identification of astrocytic SOCE. Here, using the shRNA-based gene-silencing approach and Ca^{2+}-imaging from cultured mouse astrocytes, we report that Stim1 in combination with Orai1 and Orai3 contribute to the major portion of astrocytic SOCE. Gene-silencing of Stim1 showed a 79.2% reduction of SOCE, indicating that Stim1 is the major Ca^{2+}-store-depletion-sensor. Further gene-silencing showed that Orai1, Orai2, Orai3, and TrpC1 contribute to SOCE by 35.7%, 20.3%, 26.8% and 12.2%, respectively. Simultaneous gene-silencing of all three Orai subtypes exhibited a 67.6% reduction of SOCE. Based on the detailed population analysis, we predict that Orai1 and Orai3 are expressed in astrocytes with a large SOCE, whereas TrpC1 is exclusively expressed in astrocytes with a small SOCE. This analytical approach allows us to identify the store operated channel (SOC) subtype in each cell by the degree of SOCE. Our results propose that Stim1 in combination with Orai1 and Orai3 are the major molecular components of astrocytic SOCE under various physiological and pathological conditions.

Key words: Astrocyte, SOCE, Stim1, Orai1, Orai3, TrpC1

INTRODUCTION

In the mammalian central nervous system, astrocytes constitute near 20~40% of the population of total cell number [1]. These star-like glial cells actively participate in fundamental biological processes such as maintenance of ion homeostasis, neurovascular coupling, immune response, gliotransmitter release, and metabolic

Received January 19, 2017, Revised January 31, 2017,
Accepted January 31, 2017

*To whom correspondence should be addressed.
TEL: 82-2-958-6421, FAX: 82-2-958-6919
e-mail: cjl@kist.re.kr

support of neurons [2-7]. Because these cells are electrically non-excitable, their activational and regulatory mechanisms largely depend on intracellular Ca^{2+} signaling [8-11]. It is now well established that astrocytes respond to various stimuli and signaling molecules via several Ca^{2+} signaling pathways [8, 12-14]. Among them, G protein-coupled receptor (GPCR) mediated Ca^{2+} signaling pathway is one of the most well-characterized intracellular Ca^{2+} signaling mechanisms in astrocytes [6, 15, 16]. In this signaling pathway, the Ca^{2+} stored in endoplasmic reticulum (ER) plays a key role in GPCR-mediated intracellular Ca^{2+} increase under various ligands and stimuli [14, 16, 17]. The stored Ca^{2+} is released from ER to the cytosol by an opening of IP_3R_2 channels, leading to a depletion of Ca^{2+} in ER. When the cytosolic Ca^{2+} level is elevated, the Ca^{2+} pumps in the ER membrane (SERCA) are activated to reset their cytosolic Ca^{2+} level to the basal level. During this process, however, ER reservoir remains depleted since plasma membrane Ca^{2+} APTase (PMCA) pumps Ca^{2+} out to the extracellular space much faster than the SERCA pumps Ca^{2+} into the ER store. Thus, in order to refill the ER Ca^{2+}, there must be other processes which can compensate the Ca^{2+} leakage out to the extracellular space caused by PMCAs. This is called SOCE, the mechanism that triggers influx of extracellular Ca^{2+} by gating SOCs in the plasma membrane under the ER depletion [11].

During the past decades, the idea of SOCE has become widely accepted through a series of discoveries which identified the critical components mediating SOCE: Stim1, the ER depletion sensor, and Orai or TrpC channels, the SOCs activated by Stim1 [18-20]. It has been described that during SOCE the Stim1 dimers present in ER membrane oligomerize when the ER Ca^{2+} reservoir becomes empty. Then the Stim1 oligomers physically transfer close to the plasma membrane to form a complex with SOC which is composed of either Orai or TrpC channels to open these channels [21-24].Currently, three models for SOC complexes have been proposed: "Stim1-Orai" complex, "Stim1-TrpC" complex and "Stim1-Orai/TrpC" complex [23].

So far, among the three models, the major SOC complex seems to vary depending on the cell types [23]. In astrocytes, two previous reports by Golovina group in 2005 and 2011 have revealed that astrocytic SOCE was decreased by about 70% with a gene-silencing of either TrpC1 or Orai1 [25, 26]. Therefore, according to their previous results, we can easily assume that both Orai1 and TrpC1 are equally important for astrocytic SOCE by forming "Stim1-Orai1/TrpC1" complex. However, at around the same time, Moreno group reported that both a single knock-down of Orai1 and a simultaneous knock-down of Stim1 and Orai1 resulted in a similar contribution to SOCE by nearly 50~60% [17]. Their results implied that Stim1 exclusively interacts with Orai1, supporting "Stim1-Orai1" complex model. This report was in direct conflict with Golovina group's reports. These conflicting results led us to re-examine the exact molecular mechanism mediating SOCE in astrocytes.

In this study, we have systematically investigated the relative contribution of Stim1, TrpC1 and Orai channels on SOCE to determine appropriate model for astrocytic SOC complex. To achieve this goal, we first confirmed the existence of SOCE components with previously reported mRNA transcriptome databases and our own data from qRT-PCR. Next, we developed shRNAs for various SOCE components including Stim1, Orai1, Orai2, Orai3, and TrpC1 to achieve long-lasting and reliable gene-silencing *in vitro*. After validation of the developed shRNAs, we performed ratiometric Ca^{2+} imaging to clarify the contribution of each component. Moreover, through further analyses of Ca^{2+} imaging results, we were able to subdivide the population of astrocytes into four groups depending on the size of SOCEs and characterize the features of each group. At the end, we propose the "Stim1-Orai" complex as a dominant form of astrocytic SOCE model and provide novel criteria for classifying each astrocyte by calculating "Entry/Release Ratio" from the Ca^{2+} imaging traces.

MATERIALS AND METHODS

Cell culture

Primary cortical astrocytes were prepared from 1 day postnatal C57BL/6 mice as previously described [14, 27]. The cerebral cortex was dissected free of adherent meninges, minced and dissociated into a single-cell suspension by trituration. Dissociated cells were plated onto plates coated with 0.1 mg/ml poly-D-lysine (Sigma). Cells were grown in Dulbecco's modified Eagle's medium (DMEM, Corning) supplemented with 4.5 g/L glucose, L-glutamine, sodium pyruvate, 10% heat-inactivated horse serum, 10% heat-inactivated fetal bovine serum, and 1000 units/ml of penicillin–streptomycin. Cultures were maintained at 37°C in a humidified atmosphere containing 5% CO2. After three days later, cells were vigorously washed with repeated pipetting using medium and the media was replaced to remove debris and other floating cell types.

Calcium imaging

For imaging, cultured astrocytes were plated as a monolayer on 12-mm glass coverslips coated with poly-D-lysine (Sigma). Astrocytes were incubated with 5 μM Fura-2 AM plus 1 μM pluronic acid (Molecular Probes) for 30 min at room temperature. External solution contained 150 mM NaCl, 10 mM HEPES, 3 mM KCl, 2 mM CaCl2, 1 mM MgCl2, 22 mM sucrose, and 10 mM glucose (pH adjusted to 7.4 and osmolarity to 325 mOsm).

INDEC systems, Imaging Workbench version 6.0 was used for acquisition of intensity images and conversion to ratios as previously described [28]. Thapsigargin (Tocris) was used as a sarcoendoplasmic reticulum calcium transport ATPase (SERCA) inhibitor.

shRNA development and (q)RT-PCR

The targeted genes (known RefSeq from the Pubmed) for shRNA development are mOrai1 (NM_175423.3), mOrai2 (NM_178751.3), mOrai3 (NM_198424.3), mTrpC1 (NM_011643.3), and mStim1 (NM_009287.4)

The target regions of shRNA are as the following: Orai1 candidate 1, '5'-GCAGTTCCAGGAGCTCAATGA-3"; Orai1 candidate 2, '5'-GCAACGTCCACAACCTCAACT-3"; Orai1 candidate 3, '5'-GCACCTGTTTGCCCTCATGAT-3"; Orai2 candidate 1, '5-GCTCTGCTCATCAGCACTTGC-3"; Orai2 candidate 2, '5'-GGCCACAAGGGCATGGATTAC-3"; Orai2 candidate 3, '5'-GCCACAAGGGCATGGATTACC-3"; Orai2 candidate 4, '5'-GGTAGCCGTGCATCTGTTTGC-3"; Orai3 candidate 1, '5'-GCAACATCCACAATCTCAACT-3"; Orai3 candidate 2, '5'-GGGTCAAGTTTGTGCCCATTG-3"; Orai3 candidate 3, '5'-GGGTAAACCAGCTCCTGTTGT-3"; Orai3 candidate 4, '5'-GCCCTACATTTCTACCGATCC-3"; Trpc1 candidate 1, '5'-GCTTTCGGACTTCTAAATATG-3"; Trpc1 candidate 2, '5'-CTATGGCTTAGCTACTTTGA-3"; Trpc1 candidate 3, '5'-GGGTGACTATTATATGGT-3"; Stim1 candidate 1, '5'-GCGACTTCTGAAGAGTCTACC-3"; Stim1 candidate 2, '5'-GCTGCTGGTTTGCCTATATCC-3"; and Stim1 candidate 3, '5'-GCGAGATGAGATCAACCTTGC-3".

pENSR-shRNAs for Orai1, Orai2, Orai3, Trpc1, and Stim1 were constructed by using the EZchangeTM site-directed mutagenesis kit (Enzynomics) and confirmed by sequencing.

The full-length mTrpC1 (GenBank: BC144726.1) cDNA was cloned from whole brain lysate of C57BL/6 mouse. Next, this cloned cDNA was inserted into CMV-MCS-GFP vector.

Each plasmid-based shRNA was transfected and relative transcriptome expression levels were measured by RT-PCR (TrpC1) and quantitative real-time PCR using a SYBR Green-based method (Orai1, Orai2, Orai3 and Stim1) with equal amount of cDNA. (Scrambled shRNA-containing pENSR construct was used as control.) The primer sequences for Orai1, Orai2, Orai3, Trpc1 and Stim1 transcript are as the following:

Orai1, '5'-CAGGGTTGCTCATGCTCTTT-3" & '5'-ACCGAG TTGAGGTTGTGGAC-3"; Orai2, '5'-CTGCTCATCAGCACTT GCAT-3" & '5'-GGAACTTGATCCAGCAGAGC-3"; Orai3, '5'-GGAGGTACAGCTGGAGAACG-3" & '5'-GTGTGGTGAC TGGTGGACAG-3"; Trpc1, '5'-GAATCGCGTAACCAGCTC-3" & '5'-CTTCCGGTCAGCAAAGTC-3"; and Stim1, '5'-GAGA TTGTGTCGCCCTTGTC-3" & '5'-GAGAGCTTCATCTGCAG CAC-3". And mouse GAPDH was amplified and used as the internal control.

For the KD efficiency calculation, we first normalized each mRNA level with GAPDH and divided each normalized mRNA level for Orai1 or Orai2 shRNA condition by scrambled shRNA transfected condition to calculate the apparent KD efficiency for each condition. Next, we counted the total cell number and shRNA transfected cell number to calculate the transfection efficiency, which was then used to divide the apparent KD efficiency by transfection efficiency for each condition. The resulting value was the corrected KD efficiency for Orai1 and Orai2. For the KD efficiency calculation of Orai3, TrpC1, and Stim1, we first normalized each mRNA level with GAPDH and divided each normalized mRNA level for each shRNA condition by scrambled shRNA transfected condition to calculate the apparent KD efficiency for each condition.

Data analysis and statistics

The reproduced relative mRNA expression levels of Orai1, Orai2, Orai3 and TrpC1 were obtained from the transcriptome databases of the following open access journal articles (Fig. 1b); Cahoy et al. (supplementary material:380_Cahoy_S_Table_S8_ Exon_Master_2007-09-11 [29]) and Zhang et al. (supplementary material: barreslab_rnaseq [30]).

For the definition of "Ratio" in Fig. 3b, the following formula was used;

$$\frac{"Entry"}{"Release"} = "Ratio"$$

For statistics mediating the relative SOC contribution, two way unpaired student's t-test were performed between control condition and shRNA conditions (Fig. 4b).

For relative SOC contribution calculation, we adapted the following formula (Fig. 4c);

$$\frac{(Ratio(Ctrl)\text{-}Ratio(shRNA))}{(Ratio(Ctrl))} \times 100(\%)$$

For astrocytic SOCE population analysis (Fig. 5), we displayed "Ratio" values as both frequency histogram and cumulative frequency histogram using GraphPad Prism 7.0 software. For frequency histogram, the bin size was 0.25 and for cumulative frequency histogram, the bin size was 0.01 (Fig. 5). For statistical comparison of two different cumulative frequency histograms,

https://doi.org/10.5607/en.2017.26.1.42

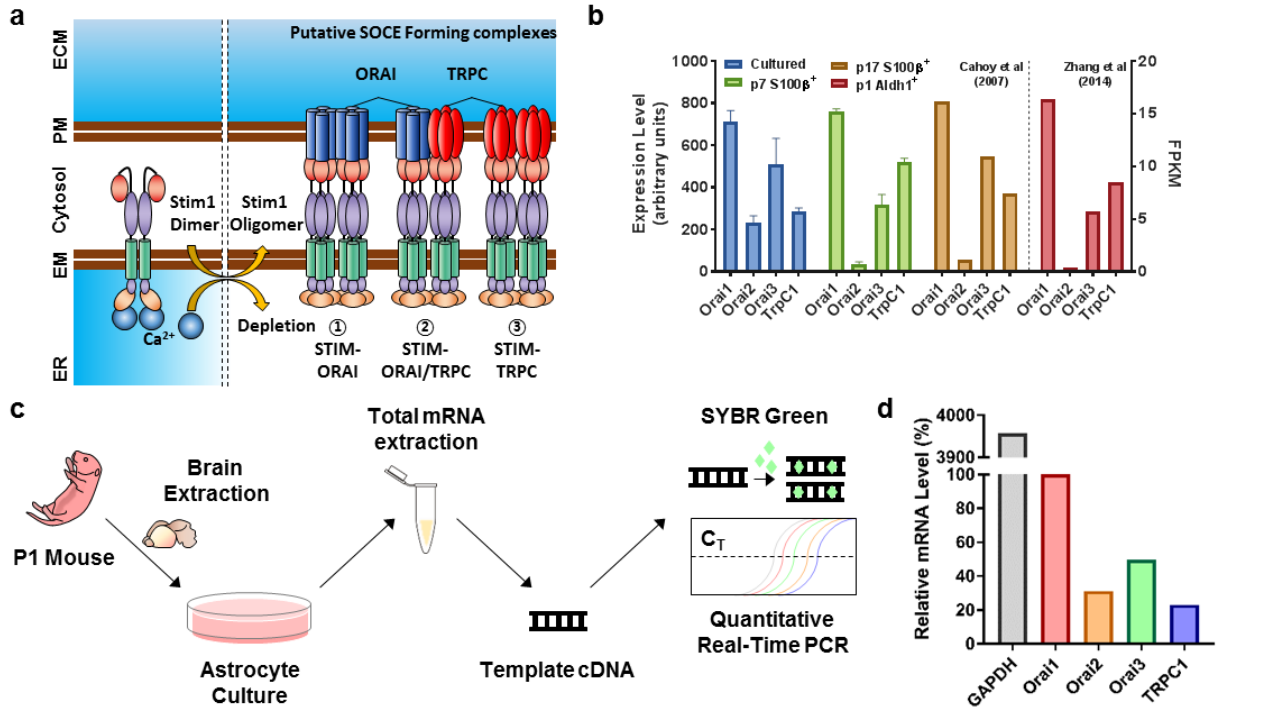

Fig. 1. Relative mRNA expression levels of SOCs in astrocytes. (a) Schematic diagram of three putative models for astrocytic SOCE components. ER Ca^{2+} depletion leads to Stim1 oligomerization and forms 1) Stim-Orai complex, 2) Stim-Orai/TrpC complex, or 3) Stim-TrpC complex. (b) Reproduced data from mRNA transcriptome database (Cahoy et al. (2008), and Zhang et al, (2014)), showing expression levels of Orai1, Orai2, Orai3, and TrpC1 in cultured astrocytes, p7 S100β$^+$ astrocytes, p17 S100β$^+$ astrocytes, and p1 Aldh1l1$^+$ astrocytes. (c) The experimental scheme of measuring mRNA levels in primary cultured 7 DIV astrocytes by quantitative real-time PCR. (d) Relative mRNA expression of Orai1(100), Orai2 (31.25), Orai3 (49.75), TrpC1 (23.12), and "Housekeeping gene" GAPDH (Glyceraldehyde 3-phosphate dehydrogenase). Orai1 expression level was arbitrary set as 100 and GAPDH was measured as a control of gene expression (3956.79).

we performed non-parametric Kolmogorov-Smirnov test (KS test) using GraphPad Prism 7.0 software (Fig. 5b~g). D and α values were estimated for calculation of significance level. This test generates the two cumulative relative frequency distributions, and then asks how far apart those two distributions are at the point where they are furthest apart. This distance is reported as Kolmogorov-Smirnov D value. For calculation of critical value, significance level of α was set 0.05.

For the fit-curve analysis (Fig. 5h), we fitted the frequency histogram of the control condition by lognormal fitting method provided by GraphPad Prsim 7.0 statistical analysis tool. From the fitted curve, statistical values of the geometric mean (GeoMean=1.31) and geometric standard deviation (GeoSD= 1.745) were calculated. Furthermore, for 95% confidence interval calculation, X_{upper}=3.899842 and X_{lower}=0.440020 were calculated by the following formula (Fig. 5h).

$$+1.96_{(p=0.05)}=\frac{ln(X_{upper})-\ln(GeoMean)}{\ln(GeoSD)}$$

$$-1.96_{(p=0.05)}=\frac{ln(X_{lower})-\ln(GeoMean)}{ln(GeoSD)}$$

For the population percentage calculations (Fig. 5h), we classified four groups based on the cut-off values: X_{lower}=0.440020, GeoMean =1.31, and X_{upper}=3.899842. Based on these cut-off values, we defined the four groups as "Small (ratio range: 0~0.625)", "Medium (ratio range: 0.625~1.375)", "Large: (ratio range: 1.375~4.125)", and "Huge: (ratio range: over 4.125)".

RESULTS

SOC subtypes are expressed in cultured mouse cortical astrocytes

In astrocytes, the exact molecular mechanism of SOCE is still unclear, and the major molecular components constituting the SOC complex need to be investigated. Therefore, we designed putative models for astrocytic SOCE: 1) Stim1-Orai complex, 2) Stim1-Orai/TrpC complex and 3) Stim1-TrpC complex (Fig. 1a). To test whether proposed molecular components

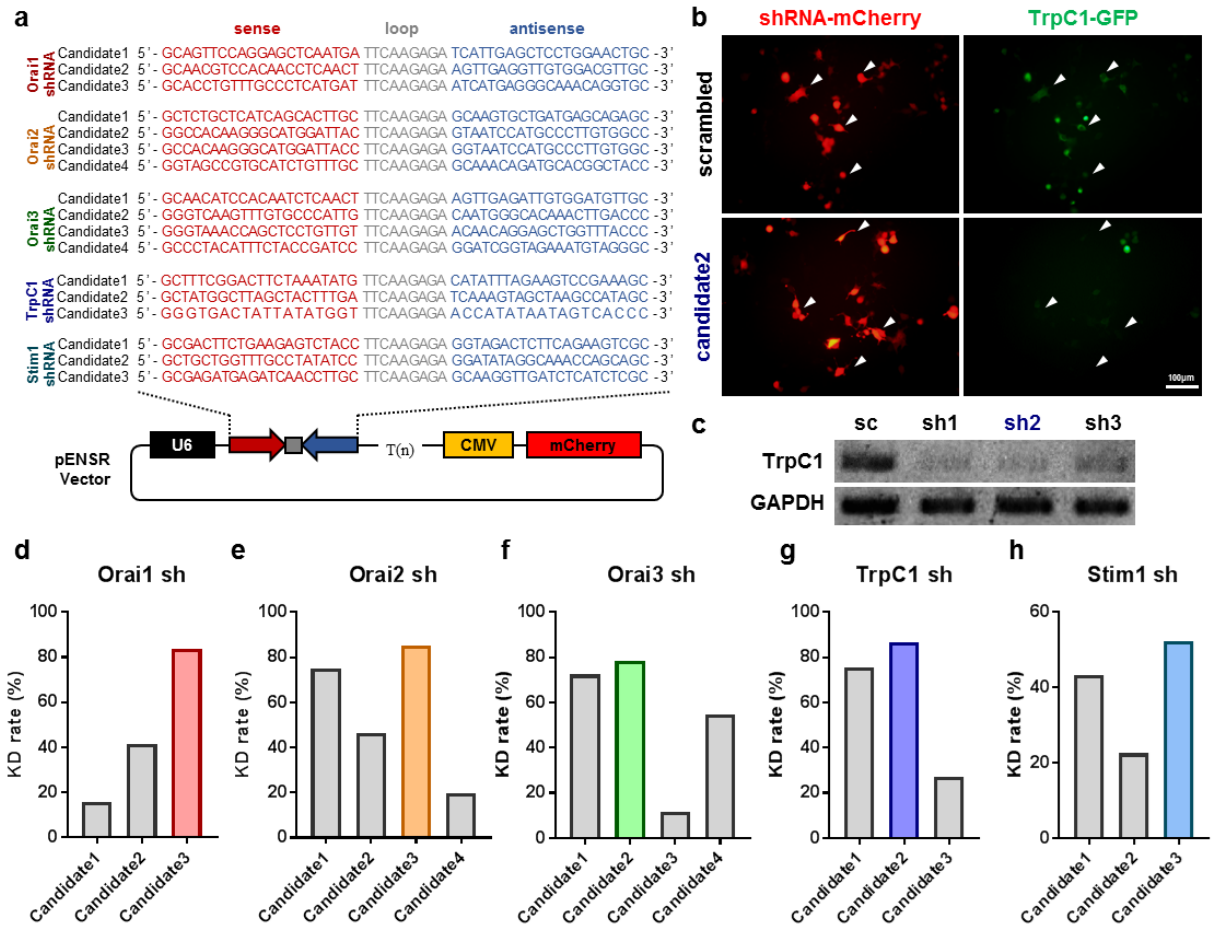

Fig. 2. Development and validation of shRNAs for SOCE components. (a) Candidate sequences for Orai1 shRNA, Orai2 shRNA, Orai3 shRNA, TrpC1 shRNA, and Stim1 shRNA are shown with vector information. Each shRNA was cloned in pENSR vector to express under U6 promoter together with a cytomegalovirus (CMV) promoter driving expression of mCherry reporter gene. (b) Fluorescence images of HEK293-T cells co-transfected TrpC1 shRNA (shRNA-mCherry) with TrpC1 full clone (TrpC1-GFP). Top, Scrambled shRNA-mCherry was co-transfected with TrpC1-GFP. Bottom, Candidate 2 of TrpC1 shRNA was co-transfected with TrpC1-GFP. (c) Quantification of TrpC1 mRNA by RT-PCR. Top, Intensity of RT-PCR bands of TrpC1 shRNA (sh1), TrpC1 shRNA 2 (sh2), TrpC1 shRNA3 (sh3) decreased. Bottom, GAPDH. (d) Knock-down rate of Orai1 shRNA candidates compared to scrambled shRNA, Candidate1: 10.4, Candidate2: 27.2, Candidate3: 54.9. (e) Knock-down rate of Orai2 shRNA candidates compared to scrambled shRNA, Candidate1: 26.9, Candidate2: 16.7, Candidate3: 30.6, Cadidate4: 7.1. (f) Knock-down rate of Orai3 shRNA candidates compared to scrambled shRNA, Candidate1: 72.3, Candidate2: 78.3, Candidate3: 11.5, Candidate4: 54.8. (g) Knock-down rate of TrpC1 shRNA candidates compared to scrambled shRNA, Candidate1: 75.6, Candidate2: 86.7, Candidate3: 27.0. (h) Knock-down rate of Stim1 shRNA candidates compared to scrambled shRNA, Candidate1: 43.2, Candidate2: 22.5, Candidate3: 52.4.

are actually present in the astrocytes, we first investigated the mRNA expression levels in astrocytes. The astrocytic mRNA transcriptome databases from the previous studies indicated that SOCs (herein Orai1, Orai2, Orai3, and TrpC1) are expressed in both *in vitro* and *in vivo* (reproduced from [29] and [30]) (Fig. 1b). In all cases, the Orai1 mRNA level was the highest, whereas the Orai2 mRNA level was the lowest.

In order to confirm whether our experimental condition exhibits similar mRNA expression pattern as the previous reports, we extracted the total mRNA from 7 days in vitro (DIV) cultured cortical astrocytes and then performed quantitative real-time RT-PCR (Fig. 1c). In our experimental condition, Orai1 showed the highest expression of mRNA level as expected, whereas TrpC1 was the lowest (Fig. 1d). In summary, both transcriptome databases and our experimental results confirmed the existence of SOC subtypes. Thus, the suggested models for astrocytic SOC complex are all possible, although the high expression level of Orai1 favored the model of "Stim1-Orai" complex.

Development and validation of shRNAs for SOCE components

In order to systematically investigate the molecular mechanism of astrocytic SOCE, we developed shRNAs for each SOCE

https://doi.org/10.5607/en.2017.26.1.42

component. Three or four candidates of shRNA sequences for Orai1, Orai2, Orai3, TrpC1, and Stim1 were selected from Invitrogen Block-iT shRNA designer website (https://rnaidesigner.thermofisher.com/) and cloned into pENSR vectors which express shRNA under the U6 promoter and fluorescent reporter (EGFP or mCherry) under the CMV promoter (Fig. 2a). After cloning of the shRNA candidates, these vectors were transfected to either astrocytes or HEK293-T cells for in vitro validation of knock-down efficiencies for each shRNA candidate. For TrpC1 shRNA validation, each TrpC1 shRNA candidate and TrpC1-GFP full clone were co-transfected into HEK293-T cells. Among the three candidates of shRNA, the candidate 2 revealed the most effective knock-down rate as indicated by a significant decrease of GFP fluorescence level and mRNA level (Fig. 2b, c).

In Orai1, Orai2, Orai3, and Stim1 shRNA development, we transfected each shRNA candidates into 7 DIV mouse cortical astrocyte and measure knock-down efficiency by the quantitative real-time PCR using a SYBR Green-based method. As a result, Candidate 3 of Orai1 shRNA, Candidate 3 of Orai2 shRNA, Candidate 2 of Orai3 shRNA, Candidate2 of TrpC1 shRNA, and Candidate 3 of Stim1 shRNA were found to be the most effective candidates respectively (Fig. 2d~h). These selected candidates were used in the Ca^{2+} imaging experiments.

Ca^{2+} imaging of astrocytic SOCE with knock-down of SOCE components

To dissect the contribution of each SOCE component in astrocytes, we performed the ratiometric Ca^{2+} imaging on Fura-2 AM loaded cultured astrocytes after gene-silencing with each shRNA (Fig. 3a). For activation of SOCE, we first applied Ca^{2+} free solution to astrocytes and treated them with 1 μM Thapsigargin (Tg), an irreversible SERCA inhibitor, to deplete the ER Ca^{2+} without any GPCR agonists. After stabilization of the baseline, we applied 2 mM Ca^{2+} solution to measure the Ca^{2+} entry. From the resulting trace, we defined the first Ca^{2+} surge as "Release" and the second Ca^{2+} surge as "Entry" (Fig. 3b). And the "Ratio" was calculated as the ratio of "Release" divided by "Entry" for each trace.

In representative Ca^{2+} imaging pictures and raw traces, both Orai1/2/3 shRNA transfected astrocyte (red marked) and control (yellow marked) showed the similar amplitude of Ca^{2+} "Release" at 3 min (3'). However, at 25 min (25') Orai1/2/3 shRNA transfected astrocyte revealed much smaller Ca^{2+} "Entry" compared to that of the control, demonstrating that Orai1/2/3 shRNA is functionally effective (Fig. 3c).

Using this experimental protocol, we measured the astrocytic SOCE after knock-down of Orai1, Orai2, Orai3, TrpC1, Orai1/2/3, and Stim1 from each astrocyte (Fig. 3d~j). The average trace of all Ca^{2+} imaging responses from individual cells for each shRNA condition with standard error mean (S.E.M) is displayed at the left side of each figure. The "Release" and "Entry" paired scatter plot and "Ratio" scatter plot was displayed on the right side of each figure (Ctrl sh: n=97, Orai1 sh: n=38, Orai2 sh: n=33, Orai3 sh: 58, TrpC1 sh: 69, Orai1/2/3 sh: n=23, Stim1 sh: n=22).

Orai1 and Orai3 channels in combination with Stim1 are the major contributors of astrocytic SOCE

To determine which model is the best fit for astrocytic SOC complex, we quantitatively analyzed the data obtained from Ca^{2+} imaging in various knock-down conditions. First, we normalized each average trace with the "Release" component for each condition and aligned and overlaid them (Fig. 4a). The maximum percent amplitude of Ctrl, TrpC1, Orai2, Orai3, Orai1, Orai1/2/3, and Stim1 knock-down conditions were 187%, 175%, 159%, 150%, 113%, 62%, and 43%, respectively (Fig. 4a). Next, we compared the average "Ratio" values of each shRNA condition with the control condition and found that Orai1, Orai3, Orai1/2/3, and Stim1 shRNA conditions were significantly different from the control shRNA condition (Fig. 4b; 2-tailed student's t-test).

To see the relative contribution of each component in astrocytic SOCE, we calculated the relative SOCE portion for each condition by subtracting the ratio value of each condition from the ratio of control condition and dividing the result by the ratio of control condition in Fig. 4b. As a result, we found that Orai1, Orai2, Orai3, TrpC1 and Stim1 contributed to SOCE by about 35.7%, 20.3%, 26.8%, 12.2% and 79.2%, respectively (Fig. 4c, d). Although there was only a slight difference between Orai2 and Orai3, the statistical significance was observed only in Orai3 ($p<0.05$) but not in Orai2 (n.s.). In summary, these results indicate that Stim1, Orai1, and Orai3 are the major contributors of the astrocytic SOCE with a statistical significance.

Identification of the SOC subtype for each astrocyte by the degree of SOCE

During the analysis of each Ca^{2+} imaging trace of the 97 cells in control condition, we noticed that the astrocytic SOCE responses were heterogeneous in regard to the "Ratio" with a pronounced scatter or variance (Fig. 3d). For instance, although most cells exhibited a "Ratio" greater than one, namely higher amplitude of "Entry" compared to "Release", some cells rather showed a "Ratio" lower than one.

To test whether this heterogeneity of astrocytic SOCE responses comes from the differential expression of SOC subtypes in astrocyte subpopulations, we performed a population analysis by plotting relative frequency and cumulative frequency histograms

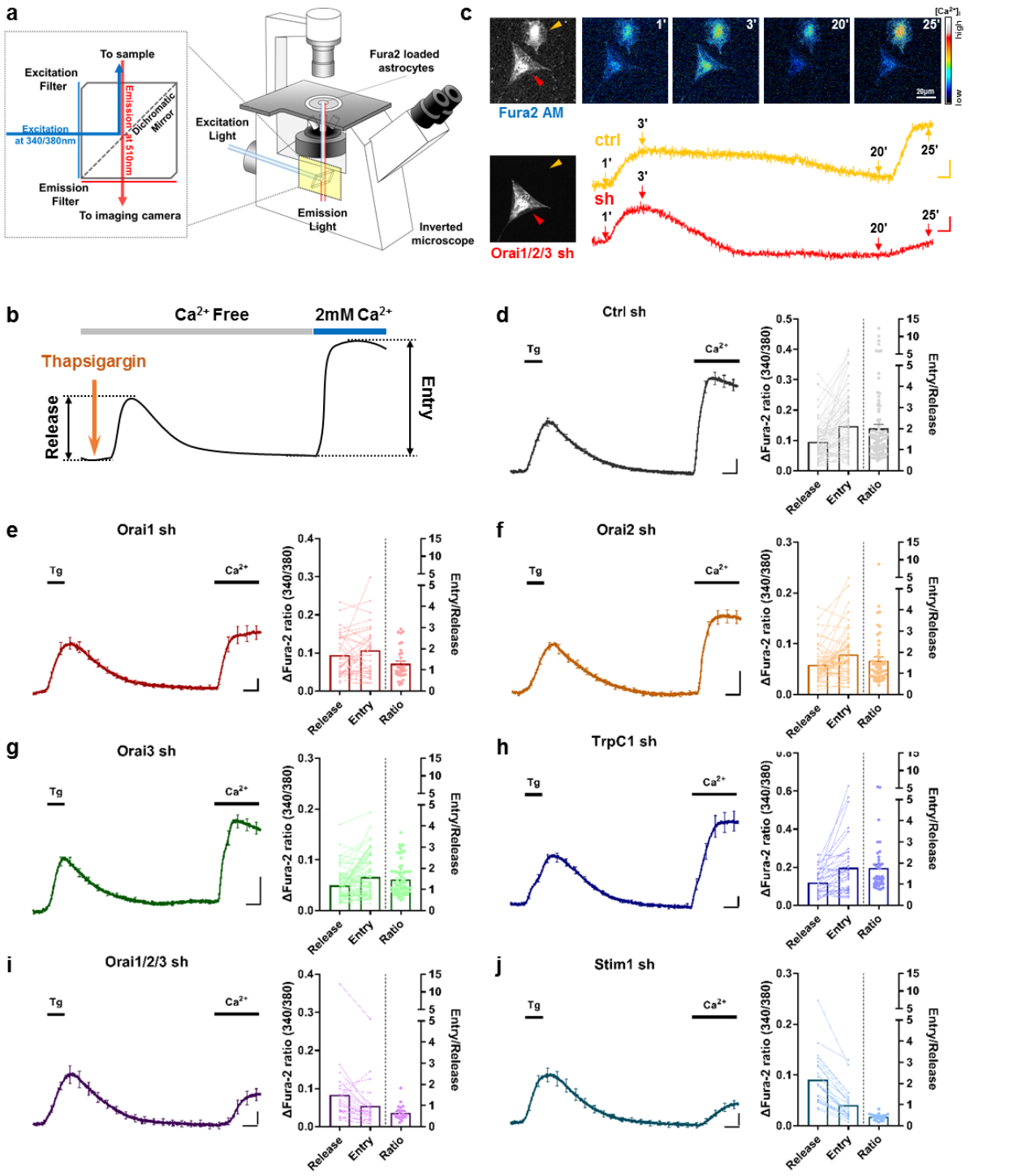

Fig. 3. Astrocytic SOCE is mediated by Orai channels in combination with Stim1. (a) Schematic illustration of astrocyte Ca^{2+} imaging in inverted microscope using ratiometric Ca^{2+} dye, Fura-2 AM. (b) Experimental protocol of Ca^{2+} imaging. Ca^{2+} free HEPES solution containing 200 nM EGTA was bath applied for 1200 s. Meanwhile, 1 μM thapsigargin, the SERCA inhibitor, was applied for 120 s after 60 s baseline to induce Ca^{2+} release from ER. External solution was changed to the normal HEPES solution containing 2 mM Ca^{2+} at 1200 s. (c) Left top, Fura-2 AM loaded cells. Left bottom, Orai1, Orai2, and Orai3 shRNA co-transfected cells expressing mCherry or EGFP. Right top, representative Ca^{2+} imaging 340/380 ratio images taken at 1 min, 3 min, 20 min, 25 min. Right bottom, representative 340/380 ratio traces of two cells. Orai1/2/3 shRNA transfected cell is indicated with red mark and endogenous control was indicated with yellow mark. (d~j) Average of total Ca^{2+} imaging traces and scatter plots of ER Ca^{2+} release (Release), store operated Ca^{2+} entry (Entry) and Entry/Release ratio (Ratio) of primary cultured astrocytes transfected with scrambled shRNA (d), Orai1 shRNA (e), Orai2 shRNA (f), Orai3 shRNA (g), TrpC1 shRNA (h), Orai1/2/3 shRNA (i), Stim1 shRNA (j). Scale bar indicates 0.5 for y axis and 100s for x axis. Tg: thapsigargin.

https://doi.org/10.5607/en.2017.26.1.42

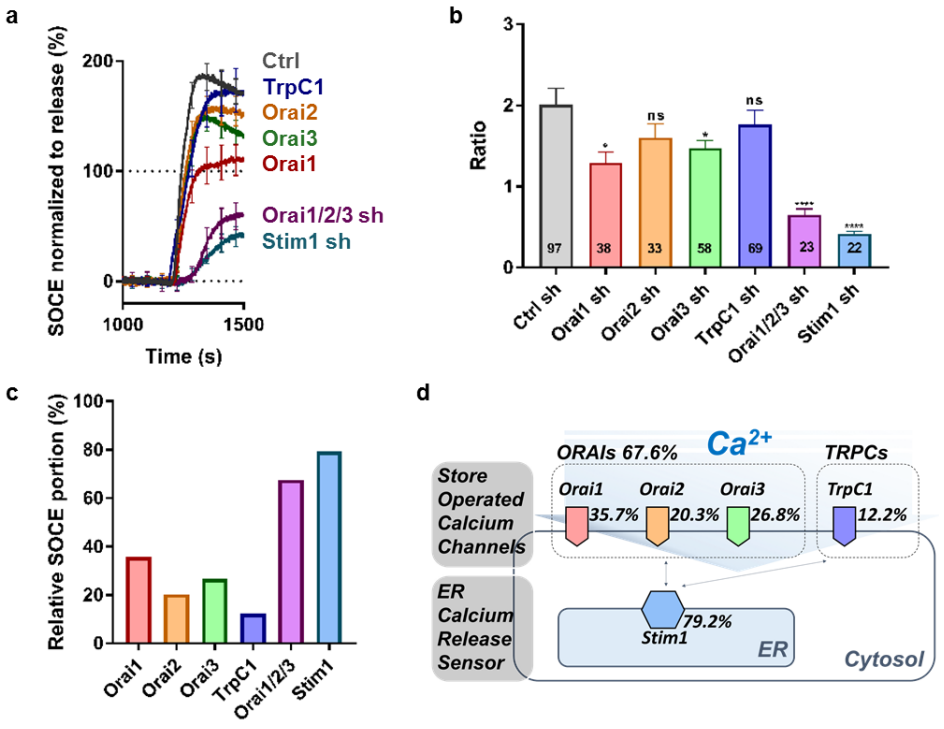

Fig. 4. Relative contribution of Stim1, Orai1, Orai2, Orai3 and TrpC1 to astrocytic SOCE. (a) Comparison of Ca^{2+} imaging traces from 1000s to 1500s normalized by amplitude of ER Ca^{2+} release. (b) Comparison of mean "Ratio" values in each condition. (c) Relative SOCE portion of each gene. 35.7% for Orai1, 20.3% for Orai2, 26.8% for Orai3, and 12.2% for TrpC1, 67.6% for Orai1/2/3 and 79.2% for Stim1. (d) Schematic diagram and summary of relative contributions. ns: not significant, *p<0.05, ****p<0.0001, student's t-test.

of the "Ratio" values (Fig. 5a~g). With this analytical method, we were able to easily compare the distribution of the "Ratio" between control condition and SOCE component knock-down conditions. As a result, we found that Stim1 and Orai1/2/3 knock-down conditions showed a dramatic shift to the left in the frequency histogram (Fig. 5f, g). At a glance, for Orai1 and Orai3 knock-down conditions the major difference occurred at large ratio values (Fig. 5c, e), whereas for Orai2 and TrpC1 knock-down conditions the frequency histograms showed a negligible difference (Fig. 5b, d).

For more in-depth analysis, we subdivided the astrocytic SOCE populations into 4 groups using statistically meaningful values. We first fitted the best non-linear lognormal curve on the frequency histogram of the control condition (Fig. 5h, top panel). Based on the fitted curve, we calculated the 95% confidential interval (upper cutoff: 0.44, lower cutoff: 3.90) and the geometric mean (1.31). With these statistically meaningful values, we defined the four subpopulations: "Small (ratio range: 0~0.625)", "Medium (ratio range: 0.625~1.375)", "Large: (ratio range: 1.375~4.125)", and "Huge: (ratio range: Over 4.125)" (Fig. 5h, For details, see Materials and Methods - Data analysis and Statistics).

With these boundary conditions, we found that each subpopulation was comprised of about 7.2% (Small), 41.2% (Medium), 42.3% (Large), and 9.3% (Huge) of astrocytic subpopulations in control condition and displayed as the population percentage plot (Fig. 5h bottom panel). We then applied the same criteria on other shRNA conditions (Fig. 5h, bottom panel). From these population percentage plots we found that knock-down of Orai1 lead to a near 2-fold increase in "Small" subpopulation and a complete disappearance of "Huge" subpopulation (Fig. 5c, h). However, silencing of Orai2 did not affect the subpopulations (Fig. 5d, h). In Orai3 shRNA condition, the subpopulations were shifted to "Medium" with a complete disappearance of "Huge" component (Fig. 5e, h). In TrpC1 shRNA condition, although overall subpopulations remained similar to the control condition, there was an unexpected disappearance of "Small" subpopulation without affecting the rest of the subpopulations (Fig. 5f, h). Simultaneous gene silencing of Orai1/2/3 lead to an almost complete disappearance of "Huge" and "Large" subpopulations, which were replaced by "Small" subpopulation. Lastly, Stim1 shRNA condition showed a disappearance of "Medium," "Large," and "Huge" subpopulations, which were replaced by 95% of "Small" subpopulation.

These results allow us to make interesting conclusions about which SOCE components are responsible for each subpopulation. For example, Orai1 and Orai3 appear to be responsible for "Large" and "Huge" subpopulations. Orai2 appears to have a minimal contribution. TrpC1 appears to be responsible for "Small" subpopulation. Stim1 appears to be responsible for "Medium", "Large," and "Huge" subpopulations, but not "Small" subpopulation. These results raise possibilities that Orai1 and Orai3 work synergistically in astrocytic SOCE to elicit Huge SOCE, and that TrpC1 serves a suppressive role in SOCE because TrpC1 shRNA

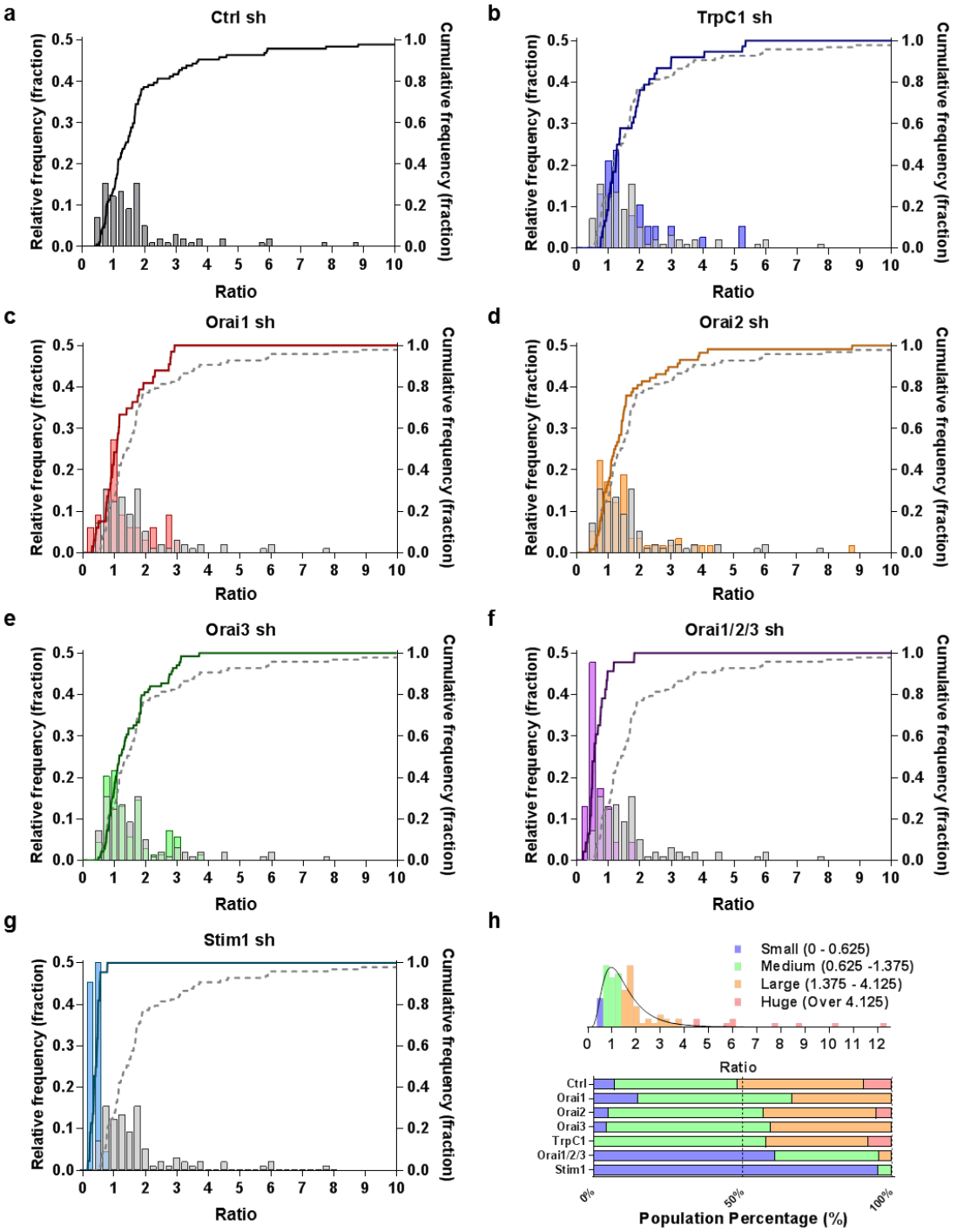

Fig. 5. Identification of the SOC subtype for each astrocyte by the degree of SOCE. (a) Relative frequency and Entry/Release ratio of control condition. (b) Comparison of relative frequency and Entry/Release ratio between control and TrpC1 shRNA. p=0.5403 (α=0.05), KS D value=0.1536. (c) Comparison of relative frequency and Entry/Release ratio between control and Orai1 shRNA. p=0.1066 (α=0.05), KS D value=0.244. (d) Comparison of relative frequency and Entry/Release ratio between control and Orai2 shRNA. p=0.1838 (α=0.05), KS D value=0.1813. (e) Comparison of relative frequency and Entry/Release ratio between control and Orai3 shRNA. p=0.4652 (α=0.05), KS D value=0.1339. (f) Comparison of relative frequency and Entry/Release ratio between control and Orai1/2/3 shRNA. p<0.0001 (α=0.05), KS D value=0.6553. (g) Comparison of relative frequency and Entry/Release ratio between control and Stim1 shRNA. p<0.0001 (α=0.05), KS D value=0.9339. (h) Fitting curve, positive skewed asymmetric Gaussian distribution of control condition with geometric mean of 1.31, geometric standard deviation of 1.745, 95% confidential interval (upper cutoff: 0.44, lower cutoff: 3.90). With these statistically meaningful values, we defined the four subpopulations: "Small(ratio range: 0~0.625)","Medium (ratio range: 0.625~1.375)","Large: (ratio range: 1.375~4.125)", and "Huge: (ratio range: Over 4.125)" (upper panel). Composition of astrocytic SOCE responses under control condition and shRNA conditions (lower panel).

https://doi.org/10.5607/en.2017.26.1.42

unmasked the "Large" subpopulation.

DISCUSSION

In summary, we have systematically investigated the astrocytic SOCE to resolve conflicting results from the previous studies [25, 26, 31]. To achieve this goal, we first determined the relative amount of mRNA of various SOCs in cultured astrocytes (Fig. 1). Then we developed and validated shRNAs for each SOCE component (Fig. 2). Using Ca^{2+} imaging we found a significant contribution of Stim1, Orai1, and Orai3 in astrocytic SOCE (Fig. 3 and 4). Finally, through the detailed population analysis of astrocytic SOCE, we developed a novel method to identify the SOC type by the degree of SOCE in each astrocyte (Fig. 5).

Through the detailed analysis of the Ca^{2+} imaging traces, we conclude that Orai1 and Orai3 are the major SOCs in cultured astrocytes. We demonstrated that among the four SOCs, Orai1 contributed the most to astrocytic SOCE in our experimental condition (35.7%; Fig. 4c, d). This value was found to be less contribution compared to the previous reports (50% in Moreno et al. 2012 and 70% in Linde et al. 2011) [17, 26]. We found that the remaining portion was attributed to Orai2 (20.3%), Orai3 (26.8%), and TrpC1 (12.2%). These proportions match well with the mRNA expression levels (Fig. 1d, 4c, 4d). Given that Orai2 and Orai3 are also *bona fide* Ca^{2} permeable channels like Orai1, it is not surprising that those proportions of each SOC type are consistent with the expression level of each SOC [32]. Therefore, both mRNA expression level and Ca^{2+} imaging results support our conclusion that Orai1 and Orai3 play the major role in astrocytic SOCE. It is possible that Orai1 and Orai3 heterodimerize like in other cells [33], and this possibility awaits for future investigation.

In regards to TrpC1 we conclude that it contributed minimally to astrocytic SOCE (12.2%, Fig. 4c, d). This was in great contrast to the previous report of about 70% contribution of astrocytic SOCE by TrpC1 [25]. This inconsistency might arise from the different gene-silencing strategy (antisense oligomer vs. shRNA), culture condition (embryonic culture of E17~18 vs. postnatal culture of P1), or type of astrocytes in culture (protoplasmic astrocytes vs. mixed culture of protoplasmic and fibrous astrocytes) between the previous study by Golovina et al. 2005 and current study. Among these differences, we speculate that the heterogeneity of astrocytic culture condition could be the most probable cause of this inconsistency. It is possible that TrpC1 is expressed in the protoplasmic astrocytes but not in the fibrous astrocytes. This possibility is supported by the low expression of TrpC1 mRNA (Fig. 1b, d), relatively small contribution of TrpC1 in astrocytic SOCE (~12.2%, Fig. 4c, d) and the disappearance of "Small" subpopulation (7.2%, Fig. 5h) by TrpC1 shRNA. Thus, it would be interesting to investigate in the future whether TrpC1 is expressed in protoplasmic astrocytes but not in fibrous astrocytes.

For the astrocytic ER depletion sensor, we conclude that Stim1 is the essential protein that mediates over 80% of astrocytic SOCE. Due to this dominant role of Stim1, it is possible that most of Orai channels interact with Stim1. These results indicate that the major astrocytic SOC complex is the Stim1-Orai complex. The remaining 20% of astrocytic SOCE might be regulated by Stim2 or other Stim1-independent mechanisms [34].

In the analysis of Ca^{2+} imaging traces, we defined and utilized the value of "Ratio," which is the ratio value of the store operated-Ca^{2+} "Entry" divided by the ER Ca^{2+} "Release," obtained from a single recording trace. "Release" component represents the Ca^{2+}-store capacity of one cell, and "Entry" component represents the ability to refill ER-Ca^{2+} from extracellular source. Thus calculating the "Ratio" might represent how fast a cell can restore its ER-Ca^{2+} storage. This normalized ratio value provides a great advantage because it minimizes the confounding contribution of artifacts and variabilities due to different experimental conditions (i.e. recording intensity), recording systems (i.e. types of the microscopes), types of Ca^{2+} indicators (i.e. Ca^{2+} dye or proteins), or ER store capacity. We propose that this entry-to-release-ratio analysis is a practical and reliable method for studying SOCE because the value of ER Ca^{2+} release depends solely on SERCA and its ER capacity, but not by SOCE component.

In the in-depth subpopulation analysis using the entry-to-release ratios, we subdivided total population into four subpopulations by statistically meaningful ratio values. This analytical method allowed us to determine which SOCE component is responsible for each subpopulation (Fig. 5h). Based on this analysis, we found two distinctive features of astrocytic SOCE. First, given that both Orai1 and Orai3 are required for "Huge" subpopulation, the combination of Orai1 and Orai3 might have a synergistic action of huge SOCE. Because the previous study revealed that the heteromeric assembly of Orai1 and 3 exhibits a decreased fast channel inactivation kinetics compared to the homomeric Orai1 [35], the similar heteromeric Orai1/3 might exist in astrocytes. Second, as TrpC1 is required for "Small" subpopulation, our results raise the interesting possibility that TrpC1 expression might have a suppressive role in mediating astrocytic SOCE. This is in contrast to our initial expectation that TrpC1 would contribute to astrocytic SOCE. Considering the fact that TrpC1 is a nonselective cation channel with much lower Ca^{2+} permeability than Orai channels [36, 37], we predict that TrpC1 competes with Orai channels to occupy the limited number of Stim1 molecules. This interesting possibility would propose TrpC1 as having a dominant

negative role. Taken together, the combinatorial interaction between the limited number of Stim1 molecules and various SOCs such as Stim1-Orai homomer, Stim1-Orai1/3 heteromer, and Stim1-Orai/TrpC1 heteromer might be the cause of the observed heterogeneity of astrocytic SOCE.

In summary, we predict that the "Small" subpopulation exhibits relatively low level of SOCE and represents TrpC1 expressing cells, whereas "Huge" subpopulation exhibits very high level of SOCE and represents both Orai1 and Orai3 expressing cells. These findings allow us to suspect the molecular profile of astrocytes in specific situation by subdividing population with our criteria of SOCE "Ratio" values. Thus, we expect that our study will provide a useful platform to understand the role of astrocytic SOCE in pathophysiology. Under pathological conditions such as Alzheimer's disease, reactive astrocytes are reported to have chronically elevated basal Ca^{2+} [38-41]. It would be interesting to investigate whether astrocytes in Alzheimer's disease express a high level of both Orai1 and Orai3. And this elevated Ca^{2+} is closely associated with the memory loss in Alzheimer's disease since reactive astrocytes release tonic form of GABA by Ca^{2+}-dependent manner, affecting the hippocampal neuronal excitability [42]. Therefore, it would be interesting to test if the Stim1-Orai complex is involved in the elevation of basal Ca^{2+}. These exciting possibilities await for future investigations.

ACKNOWLEDGEMENTS

This study was supported by Creative Research Initiative Program, Korean National Research Foundation (2015R1A3A2066619), KIST Institutional Grant (2E26662), and KU-KIST Graduate School of Science and Technology program (R1435281).

REFERENCES

1. Khakh BS, Sofroniew MV (2015) Diversity of astrocyte functions and phenotypes in neural circuits. Nat Neurosci 18:942-952.
2. Perea G, Araque A (2010) GLIA modulates synaptic transmission. Brain Res Rev 63:93-102.
3. Panatier A, Vallée J, Haber M, Murai KK, Lacaille JC, Robitaille R (2011) Astrocytes are endogenous regulators of basal transmission at central synapses. Cell 146:785-798.
4. Suzuki A, Stern SA, Bozdagi O, Huntley GW, Walker RH, Magistretti PJ, Alberini CM (2011) Astrocyte-neuron lactate transport is required for long-term memory formation. Cell 144:810-823.
5. Ransom BR, Ransom CB (2012) Astrocytes: multitalented stars of the central nervous system. Methods Mol Biol 814:3-7.
6. Woo DH, Han KS, Shim JW, Yoon BE, Kim E, Bae JY, Oh SJ, Hwang EM, Marmorstein AD, Bae YC, Park JY, Lee CJ (2012) TREK-1 and Best1 channels mediate fast and slow glutamate release in astrocytes upon GPCR activation. Cell 151:25-40.
7. Lee S, Yoon BE, Berglund K, Oh SJ, Park H, Shin HS, Augustine GJ, Lee CJ (2010) Channel-mediated tonic GABA release from glia. Science 330:790-796.
8. Bazargani N, Attwell D (2016) Astrocyte calcium signaling: the third wave. Nat Neurosci 19:182-189.
9. Shigetomi E, Patel S, Khakh BS (2016) Probing the complexities of astrocyte calcium signaling. Trends Cell Biol 26: 300-312.
10. Rusakov DA (2015) Disentangling calcium-driven astrocyte physiology. Nat Rev Neurosci 16:226-233.
11. Clapham DE (2007) Calcium signaling. Cell 131:1047-1058.
12. Volterra A, Liaudet N, Savtchouk I (2014) Astrocyte Ca^{2+} signalling: an unexpected complexity. Nat Rev Neurosci 15: 327-335.
13. Shigetomi E, Tong X, Kwan KY, Corey DP, Khakh BS (2011) TRPA1 channels regulate astrocyte resting calcium and inhibitory synapse efficacy through GAT-3. Nat Neurosci 15:70-80.
14. Lee J, Chun YE, Han KS, Lee J, Woo DH, Lee CJ (2015) Ca(2+) entry is required for mechanical stimulation-induced ATP release from astrocyte. Exp Neurobiol 24:17-23.
15. Oh SJ, Han KS, Park H, Woo DH, Kim HY, Traynelis SF, Lee CJ (2012) Protease activated receptor 1-induced glutamate release in cultured astrocytes is mediated by Bestrophin-1 channel but not by vesicular exocytosis. Mol Brain 5:38.
16. Nakahara K, Okada M, Nakanishi S (1997) The metabotropic glutamate receptor mGluR5 induces calcium oscillations in cultured astrocytes via protein kinase C phosphorylation. J Neurochem 69:1467-1475.
17. Moreno C, Sampieri A, Vivas O, Peña-Segura C, Vaca L (2012) STIM1 and Orai1 mediate thrombin-induced Ca(2+) influx in rat cortical astrocytes. Cell Calcium 52:457-467.
18. Zhang SL, Yu Y, Roos J, Kozak JA, Deerinck TJ, Ellisman MH, Stauderman KA, Cahalan MD (2005) STIM1 is a Ca2+ sensor that activates CRAC channels and migrates from the Ca2+ store to the plasma membrane. Nature 437:902-905.
19. Prakriya M, Feske S, Gwack Y, Srikanth S, Rao A, Hogan PG (2006) Orai1 is an essential pore subunit of the CRAC channel. Nature 443:230-233.
20. Ambudkar IS, Ong HL, Liu X, Bandyopadhyay BC, Cheng KT (2007) TRPC1: the link between functionally distinct

store-operated calcium channels. Cell Calcium 42:213-223.
21. Liao Y, Erxleben C, Abramowitz J, Flockerzi V, Zhu MX, Armstrong DL, Birnbaumer L (2008) Functional interactions among Orai1, TRPCs, and STIM1 suggest a STIM-regulated heteromeric Orai/TRPC model for SOCE/Icrac channels. Proc Natl Acad Sci U S A 105:2895-2900.
22. Ong HL, Cheng KT, Liu X, Bandyopadhyay BC, Paria BC, Soboloff J, Pani B, Gwack Y, Srikanth S, Singh BB, Gill DL, Ambudkar IS (2007) Dynamic assembly of TRPC1-STIM1-Orai1 ternary complex is involved in store-operated calcium influx. Evidence for similarities in store-operated and calcium release-activated calcium channel components. J Biol Chem 282:9105-9116.
23. Collins HE, Zhu-Mauldin X, Marchase RB, Chatham JC (2013) STIM1/Orai1-mediated SOCE: current perspectives and potential roles in cardiac function and pathology. Am J Physiol Heart Circ Physiol 305:H446-H458.
24. Pani B, Ong HL, Brazer SC, Liu X, Rauser K, Singh BB, Ambudkar IS (2009) Activation of TRPC1 by STIM1 in ER-PM microdomains involves release of the channel from its scaffold caveolin-1. Proc Natl Acad Sci U S A 106:20087-20092.
25. Golovina VA (2005) Visualization of localized store-operated calcium entry in mouse astrocytes. Close proximity to the endoplasmic reticulum. J Physiol 564:737-749.
26. Linde CI, Baryshnikov SG, Mazzocco-Spezzia A, Golovina VA (2011) Dysregulation of Ca2+ signaling in astrocytes from mice lacking amyloid precursor protein. Am J Physiol Cell Physiol 300:C1502-C1512.
27. Hwang EM, Kim E, Yarishkin O, Woo DH, Han KS, Park N, Bae Y, Woo J, Kim D, Park M, Lee CJ, Park JY (2014) A disulphide-linked heterodimer of TWIK-1 and TREK-1 mediates passive conductance in astrocytes. Nat Commun 5:3227.
28. Kang SS, Han KS, Ku BM, Lee YK, Hong J, Shin HY, Almonte AG, Woo DH, Brat DJ, Hwang EM, Yoo SH, Chung CK, Park SH, Paek SH, Roh EJ, Lee SJ, Park JY, Traynelis SF, Lee CJ (2010) Caffeine-mediated inhibition of calcium release channel inositol 1,4,5-trisphosphate receptor subtype 3 blocks glioblastoma invasion and extends survival. Cancer Res 70:1173-1183.
29. Cahoy JD, Emery B, Kaushal A, Foo LC, Zamanian JL, Christopherson KS, Xing Y, Lubischer JL, Krieg PA, Krupenko SA, Thompson WJ, Barres BA (2008) A transcriptome database for astrocytes, neurons, and oligodendrocytes: a new resource for understanding brain development and function. J Neurosci 28:264-278.
30. Zhang Y, Chen K, Sloan SA, Bennett ML, Scholze AR, O'Keeffe S, Phatnani HP, Guarnieri P, Caneda C, Ruderisch N, Deng S, Liddelow SA, Zhang C, Daneman R, Maniatis T, Barres BA, Wu JQ (2014) An RNA-sequencing transcriptome and splicing database of glia, neurons, and vascular cells of the cerebral cortex. J Neurosci 34:11929-11947.
31. Moreno C, Vaca L (2011) SOC and now also SIC: store-operated and store-inhibited channels. IUBMB Life 63:856-863.
32. Gwack Y, Srikanth S, Feske S, Cruz-Guilloty F, Oh-hora M, Neems DS, Hogan PG, Rao A (2007) Biochemical and functional characterization of Orai proteins. J Biol Chem 282:16232-16243.
33. Zhang X, Zhang W, González-Cobos JC, Jardin I, Romanin C, Matrougui K, Trebak M (2014) Complex role of STIM1 in the activation of store-independent Orai1/3 channels. J Gen Physiol 143:345-359.
34. Lee KP, Yuan JP, So I, Worley PF, Muallem S (2010) STIM1-dependent and STIM1-independent function of transient receptor potential canonical (TRPC) channels tunes their store-operated mode. J Biol Chem 285:38666-38673.
35. Schindl R, Frischauf I, Bergsmann J, Muik M, Derler I, Lackner B, Groschner K, Romanin C (2009) Plasticity in Ca2+ selectivity of Orai1/Orai3 heteromeric channel. Proc Natl Acad Sci U S A 106:19623-19628.
36. Liao Y, Abramowitz J, Birnbaumer L (2014) The TRPC family of TRP channels: roles inferred (mostly) from knockout mice and relationship to ORAI proteins. Handb Exp Pharmacol 223:1055-1075.
37. Vig M, Beck A, Billingsley JM, Lis A, Parvez S, Peinelt C, Koomoa DL, Soboloff J, Gill DL, Fleig A, Kinet JP, Penner R (2006) CRACM1 multimers form the ion-selective pore of the CRAC channel. Curr Biol 16:2073-2079.
38. Popugaeva E, Vlasova OL, Bezprozvanny I (2015) Restoring calcium homeostasis to treat Alzheimer's disease: a future perspective. Neurodegener Dis Manag 5:395-398.
39. Zhang H, Sun S, Wu L, Pchitskaya E, Zakharova O, Fon Tacer K, Bezprozvanny I (2016) Store-operated calcium channel complex in postsynaptic spines: a new therapeutic target for Alzheimer's disease treatment. J Neurosci 36:11837-11850.
40. Wu J, Ryskamp DA, Liang X, Egorova P, Zakharova O, Hung G, Bezprozvanny I (2016) Enhanced store-operated calcium entry leads to striatal synaptic loss in a Huntington's disease mouse model. J Neurosci 36:125-141.
41. Kuchibhotla KV, Lattarulo CR, Hyman BT, Bacskai BJ (2009) Synchronous hyperactivity and intercellular calcium waves in astrocytes in Alzheimer mice. Science 323:1211-1215.

42. Jo S, Yarishkin O, Hwang YJ, Chun YE, Park M, Woo DH, Bae JY, Kim T, Lee J, Chun H, Park HJ, Lee DY, Hong J, Kim HY, Oh SJ, Park SJ, Lee H, Yoon BE, Kim Y, Jeong Y, Shim I, Bae YC, Cho J, Kowall NW, Ryu H, Hwang E, Kim D, Lee CJ (2014) GABA from reactive astrocytes impairs memory in mouse models of Alzheimer's disease. Nat Med 20:886-896.

 https://doi.org/10.5607/en.2017.26.1.42